INTERNATIONAL ATOMIC ENERGY AGENCY
UNITED NATIONS EDUCATIONAL, SCIENTIFIC AND CULTURAL ORGANIZATION
INTERNATIONAL CENTRE FOR THEORETICAL PHYSICS
I.C.T.P., P.O. BOX 586, 34100 TRIESTE, ITALY. CABLE: CENTRATOM TRIESTE

SMR.769 - 2

WORKSHOP ON "NON-LINEAR ELECTROMAGNETIC INTERACTIONS IN SEMICONDUCTORS"

1 - 10 AUGUST 1994

"Electro-optical non-linear processes in superlattices and low power optical bistabilities"

P. VOISIN
Department of Physique
Ecole Normale Superieure
24 Rue L'Homond
F-75005 Paris
FRANCE

Examples of giant resonant optical non-linearities:

1) high efficiency photon energy up-conversion by an "Auger fountain" at InP-AlInAs type II interfaces
2) low threshold optical bistability in InGaAs-AlInAs superlattice p-i-n diodes

Paul Voisin

Laboratoire de Physique de la Matière Condensée de l'Ecole Normale Supérieure
24 rue Lhomond, F 75005 Paris

Photon energy conversion and bistability are two major concerns of non-linear optics. The analysis of optical non-linearities usually relies on a power expansion of the polarisation in function of the electric fields in the form:

$$P = X(1) : E + X(2) : E\,E + X(3) : E\,E\,E \qquad (1)$$

where X(n) is the nth order susceptibility tensor, of rank n+1. This expansion naturally points to the group-theoretical analysis of the crystal symetries and light beams geometry. Far from absorption resonances, the non-linear susceptibilities are relatively small and non-linear effects become important when the applied (static or light wave) electric field becomes non-negligible compared to the internal electric fields associated with chemical bonds, which requires very large excitation intensities allowed only by short pulse lasers. Also, it is clear that Eq. 1 implicitely applies more naturally to the situation of coherent excitation.

However, there are many circumstances where optical non-linearities arise from resonant physical processes. In this case, symmetry rules are often violated, the coherence of light waves becomes unimportant, and the power expansion Eq(1) may be irrelevant to the analysis of the phenomena. A completely trivial example is photo-luminescence where the energy of the pump

photon is converted downward into the emitted photon, which might be considered as an incoherent optical non-linearity. In these lectures, I shall discuss two distinct topics which have this unique common feature that they are huge (non trivial) non-linearities associated with resonantly excited photo-carriers. The first effect deals with photon energy up-conversion, which is a quite uncommon phenomenon under the moderate excitation conditions usually found in a cw experiment. Paradoxally, this high efficiency up-conversion is associated with an usually undesired non-radiative recombination chanel, the Auger effect. The second topic adresses the problem of optical bistability. Usually, bistability is obtained in a Fabry-Pérot cavity containing a medium whose optical index depends on the light intensity. The interplay between the cavity resonance condition (depending on the optical index) and the light intensity in the cavity (which acts on the optical index) may in chosen circumstances lead to bistable behavior where the Fabry-Pérot switches hysteretically, for instance from a low power-high reflectivity state to a high power-low reflectivity state. On the other hand, low power optical bistability has been observed in electro-optical devices where a feed-back mechanism couples the optical absorption and the electric field across the devices, which affects the absorption via the electro-optical response. These devices, invented by DAB Miller at Bell Labs in 1985 and named SEEDs (self electro-optical effect devices), have been considerably developped over the last ten years. However, SEEDs require an individual electrical circuit and/or differential illumination which hampers their use in very large scale matrices because of the complexity of interconnexions. I shall discuss the feasability of a "wireless" SEED based on the interplay between a sensitive electro-optical effect, the Wannier-Stark effect in semiconductor superlattices, and the screening of the built-in electric field by the photocarriers in a p-i-n diode. Projections of our results for the case of small pixels lead us to anticipate that these devices would display all-optical bistability with an extremely low commutation energy (about ten femto-Joule), actually close to the physical limit, and comparable to the present commutation energy of C-MOS transistors.

These lecture notes consist of two original papers recently published on these two topics. I hope that they are sufficiently self-contained to serve as a useful written support to the lectures given at this workshop on non-linear optical interactions in semiconductors.

High efficiency energy up-conversion by an "Auger fountain" at an InP-AlInAs type II heterojunction

W. Seidel, A. Titkov°, J.P. André*, P. Voisin and M. Voos

Laboratoire de Physique de la Matière Condensée de l'Ecole Normale Supérieure
24 rue Lhomond, F75005 Paris, France

*Laboratoire d'Electronique Philips
23 Av. Descartes, F94453 Limeil-Brévannes, France

Abstract:

Luminescence of bulk InP at 1.41 eV is observed when photo-exciting a type II InP-AlInAs single heterojunction above the spatially indirect bandgap at 1.23 eV. This energy up-conversion effect, which is extremely efficient even at moderate pump power, is due to a "Auger fountain" mechanism producing high energy holes which redistribute over the heterostructure and recombine with native electrons in the InP layer. The analysis of this phenomenon suggests technological applications as well as analogies with other fields like photo-chemistry.

PACS codes: 73.20.Dx, 78.65.Fa, 42.65.Ky

Photon energy up-conversion, like perpetual motion, seems to be a challenge to thermodynamics. Most energy up-conversion effects, like the anti-Stokes lines in Raman spectroscopy, rely on the existence of a hot reservoir, for instance thermal population of the phonon modes, and the amount of energy which can be up-converted is of the order of kT. Another example is nuclear fusion, which requires very hot plasmas to overcome the Coulomb potential barrier. "Cold" processes do exist, like second harmonic generation or two-photon sequential absorption[1] in non linear optics, but they are usually quite unefficient at the moderate pump power found in a cw experiment. In this Letter, we report on an energy up-conversion effect which is both "cold" and astonishingly efficient under cw excitation conditions usual in semiconductor physics. Paradoxally, this effect is linked to Auger recombination, which is better known as a non-radiative process and a fundamental limitation to the efficiency of semiconductor lasers[2]. The way the "Auger fountain" works is the following: an Auger recombination event involving one electron and two holes leaves a high energy hole, which, during thermalization, is redistributed in k-space (e.g. a different band) or in real space[3] (e.g. a different part of the sample). If the final state is metastable enough, this hole is available for a radiative recombination at an energy possibly higher than the pump energy. A very weak luminescence from the spin-orbit split-off band has indeed been observed in the past in bulk GaSb[4], and attributed to such a mechanism. Luminescence up-conversion due to inter-Landau level excitations by Auger process in a doped quantum well have also been reported[5]. As we evidence below, the restricted conditions for a high efficiency can be found in a type II heterostructure where the heterojunction electric field drifts the Auger hole into the "barrier" material and avoids its thermalization in the fundamental level. Type II heterostructures offer a completely original situation with respect to radiative as well as Auger recombinations, since electrons and holes are spatially separated and recombination allowed only by the small overlap of the wavefunction tails outside the potential wells where they are localized. Recently, we started the investigation of InP-AlInAs heterostructures, which are the most regular among the type II systems

fabricated so far, with electrons localized in InP and holes in AlInAs. This study revealed several interesting features, like the non-commutativity of band discontinuities[6] or an unexpected low threshold laser emission[7]. Here, we report on luminescence energy up-conversion by the Auger fountain mechanism in a InP-AlInAs single heterojunction[8].

Our sample was grown by Metal-Organic Chemical Vapor Deposition on a n-doped InP substrate. As shown in Fig. 1a, this heterostructure simply consists of a 1000 Å thick InP buffer layer, with a low n-type residual doping in the 10^{14} cm^{-3} range, followed by a 1000 Å thick AlInAs layer with a n-type residual doping in the 10^{16} cm^{-3} range. The free surface is protected by a 50 Å InGaAs layer. Calculation of the charge transfer at the interface[9] for a conduction band offset equal to 470 meV[6] and an AlInAs doping level $N_D = 2.\ 10^{16}$ cm^{-3} yields a two-dimensional electron gas (TDEG) with an areal density $n_S = 3.\ 10^{11}$ cm^{-2}. The electric field at the interface is 30 kV/cm. Electron and heavy hole confinement energies in their respective quasi-triangular quantum wells are 30 meV and 20 meV respectively. The low temperature photoluminescence (PL) spectrum under low power excitation by a He-Ne laser is shown in Fig. 1b. A strong line "A" corresponding to recombination at the type II interface is observed at 1.23 eV. The PL from the InP buffer layer shows up as a sharp line "B" at 1.41 eV, emerging from a broad background "C" due to the substrate. A weaker PL line "D" from the AlInAs layer appears at 1.63 eV, which corresponds to a 4% Al-rich composition with respect to the alloy lattice matched to InP. Excitation (PLE) spectra[10] of these lines (dashed lines in Fig. 1b) show directly the corresponding absorption gaps. It is remarkable that the gap associated with the interface can be observed directly from the excitation spectrum of the "A" line in spite of the very small absorption associated with the type II single heterojunction.

We now discuss results obtained using a Ti:Sapphire tunable laser with a power of a few tens of mW and loosely focused on the sample using a long focal (f=0.8 m) lens, which gives a beam waist of 1 mm. For an excitation energy above the InP bandgap ($h\nu_1 = 1.51$ eV), the PL spectrum shows very little dependence on

the excitation power: the lineshapes do not change appreciably and, as shown in Fig. 2a, the nearly identical integrated intensities of the "A" and "B" lines vary linearly with the pump power over several decades. This proves that the radiative efficiencies are essentially constant for this range of excitation densities. However, when the sample is excited at $h\nu_2$=1.325 eV, i.e. between the interface and InP bandgaps, a rather unusual feature is observed: as shown in Fig. 1c, the luminescence from the InP buffer layer can still be observed, although much weaker than before. As can be seen on Fig. 2b, this "B" line now has a quadratic dependence on the excitation power I, while the "A" line still shows the linear variation. As we ensured a perfect spectral filtering of the laser beam, this InP luminescence clearly corresponds to an up-conversion of the exciting photon energy. To discriminate between possible explanations like two-photon absorption, intra-band absorption by photo-carriers etc..., we have examined the wavelength dependence of the effect at a fixed pump intensity, which amounts to measure an "anti-PLE" spectrum of an anti-Stokes PL line. We find that the signal varies exactly like the square of the interface absorption α^A determined by the normal PLE spectrum of the "A" line (Fig. 1b). As in these experimental conditions the areal density of photocarriers is much lower than the TDEG density, this result proves that the up-converted signal is directly proportional to the photo-hole density p_S. The only mechanism which immediately explains both the $(I)^2$ and the $(\alpha^A)^2$ dependences is the "fountain" effect due to Auger process involving a native electron and two photo-holes, as sketched in Fig. 1a: those of the high energy Auger holes which fall towards the InP side are pushed away from the interface by the heterojunction electric field. They thermalize at the top of InP valence band and recombine there with native electrons.

This effect is easily modeled using simple rate equations. With the superscripts A, B refering to the interface and InP luminescences and the subscripts 1, 2 refering to the excitation energies 1.51 eV and 1.325 eV, we write four equations in the form:

$$L^{A,B}{}_{1,2} = g\eta^{A,B}\, G^{A,B}{}_{1,2} \qquad (1)$$

where L is the signal intensity, G the corresponding generation rate, η the radiative efficiency and g an external coupling constant. For photo-carriers, we have:

$$G_{ph} = \alpha\, I\, (1-R) / h\nu \qquad (2)$$

where α (dimensionless) is the related absorption (i.e. the fraction of incident photons absorbed by the corresponding transitions), $R \approx 0.3$ the sample reflectivity and $h\nu$ the exciting photon energy. For the Auger carriers fed to InP, we write, in formal analogy with the bulk situation:

$$G_{Auger} = 0.5\, S\, C_p\, n_S\, p_S^2 \qquad (3)$$

where S is the surface of the excited region. C_p is the two dimensional equivalent of the usual Auger coefficient. The 0.5 factor accounts for the fact that only half of the Auger holes fall toward InP. As already mentioned, n_S is essentially equal to the density of native electrons in the TDEG. Finally, if the radiative part of the interface recombination follows an exponential law with a time constant τ^A, we have (assuming that the Auger holes falling towards AlInAs are fed back to the interface) :

$$d/dt\, S\, p_S = G_{ph} - S\, p_S / \tau^A - 2\, G_{Auger} \qquad (4)$$

Our investigations of the luminescence decay, using a cavity dumped Ar^+ laser at low power, yield τ^A=15 ns. As this value is comparable with the pulse duration, we cannot establish directly that the decay follows a simple exponential law, but this assumption is clearly supported by the observation of a linear kinetics under these excitation conditions.

As long as G_{Auger} remains negligible, this set of equations predicts the observed dependences of L^{A}_1, L^{B}_1, L^{A}_2 and L^{B}_2 on the excitation intensity I and the related absorptions. Using $n_S = 3.\ 10^{11}$ cm^{-2}, $\alpha^{B}_1 = 0.1$ for the absorption by the 1000Å thick InP buffer layer, and $\alpha^{A}_1 / \alpha^{A}_2 = 5.5$ as measured directly on the extended PLE spectrum of the "A" line, the combination of the experimental data yields $C_p\ (\alpha^{A}_2)^2 = 3.2\ 10^{-20}$ cm^{4}s^{-1}.

At this stage, further elucidation of the situation has to rely on a calculation of the interface absorption α^{A}. This is done by solving numerically the Schrödinger equation for the envelope functions in the potential sketched in the insert of Fig.3, using a transfer matrix method. While the threshold absorption depends considerably on the actual parameters (electric field at the interface and depth of the triangular quantum well), we observe that, as a consequence of an effective sum rule, the calculated absorption at 1.32 eV, about 80 meV above the interface bandgap, remains nearly constant and equal to 10^{-4}. However, this result can be changed considerably and in both directions by simulating equally plausible imperfections of the interface: by adding two monolayers of InAs at the interface, as suggested by the results of Brasil et al.[11], we get an absorption ten time larger (spectrum "b" in Fig. 3), while by simulating a 30 Å-wide graded interface, we get an absorption about 50% smaller (spectrum "c" in Fig. 3). The strong absorption with quasi parabolic profile above 1.42 eV corresponds to direct transitions in the 1000 Å thick InP layer forming the left part of the structure. It does not depend on the modeling of the interface potential and yields the expected value. Using $\alpha^{A}_2 = 10^{-4}$, and the data for I=100 mW at $h\nu_2$, we get $C_p = 3.2\ 10^{-12}$ cm^4 s^{-1}, and $p_S = 6.10^7$ cm^{-2} . Hence, p_S is always negligible compared to the density of native electrons, which explains why the luminescence lineshape, line position and lifetime are constant in our range of laser excitation.

To complete this study, we then investigate the saturation of the up-conversion effect by increasing the excitation density, using a tighter focusing (f=50 mm) and a slightly shorter wavelength ($h\nu_3$= 1.375 eV) where more power is available from the Ti:Sapphire laser. The interface absorption at $h\nu_3$ is also

somewhat larger, as $\alpha^{A}_3/\alpha^{A}_2= 1.33$. We show in Fig. 4 the ratio of the InP and interface luminescences L^{B}_3 / L^{A}_3 as a function of the laser intensity, together with fits using Eqs. 1-4. At "low" power, we find again the quadratic and linear dependences, which yield about the same value of $C_p(\alpha^{A})^2$ as before. At higher excitation, the up-converted luminescence tends to become linear, and the interface luminescence saturates as $I^{1/2}$. This regime rather measures the value of $C_p(\alpha^{A})^3$, hence we now have a complete solution, giving $C_p = 3.9\ 10^{-12}\ cm^4s^{-1}$ and $\alpha^{A}_3 = 1.9\ 10^{-4}$ (dotted line in Fig. 4) or $C_p = 4.6\ 10^{-11}\ cm^4s^{-1}$ and $\alpha^{A}_3 = 0.73\ 10^{-4}$ (dashed line in Fig. 4). The first set of values, which gives a better agreement with the loose focusing results, is clearly more satisfactory, as other saturation mechanisms (heating !) can explain the deviation of the highest excitation data from our simple model. Given the simplicity of the model and the range of experimental data, the agreement is rather fair. The figure for α^{A} indicates a nearly ideal interface, which might be the strangest part of our results. Another surprise is the value of the Auger coefficient: a natural, although completely arbitrary scaling of the electron and hole densities by the extension of their wavefunctions along the z axis allows a reduction to an "equivalent three dimensional Auger coefficient" which turns out to be about three orders of magnitude larger than the values usually reported for small spin-orbit bulk III-V semiconductors or type I quantum wells[4,12,13]. This seems at odd with the observation of fair laser effect in InP-AlInAs superlattices[6].

Finally, if we take into account the considerable difference between the interface and InP radiative efficiencies $\eta^{A}/\eta^{B} \approx 100$ (which is evidenced directly by the nearly equal luminescence intensities at $h\nu_1 = 1.51$ eV, in spite of the $\approx$1:100 absorption ratio), our high excitation data show that the up-conversion process reaches a nearly total efficiency (half of the pump photons up-converted) at an excitation density of the order of 10 kW / cm^2, which is an amazingly small intensity for non-linear optics. This points out to possible applications: by appropriate bandgap engineering (e.g. by deliberate addition of a thin InAs layer), it should be possible to lower the interface bandgap down towards half the InP bandgap and increase the

energy conversion up to about 700 meV. As at the same time the interface absorption would increase, this might open interesting perspectives for infrared image conversion. Also, it is noteworthy that the main ingredient of this new Auger fountain effect, which is the spatial separation of the ground and excited states avoiding the thermalization of the Auger carriers, may be found in other systems like organic molecules. This suggests the possibility of analogous effects in photo-chemistry.

In conclusion, we have observed high efficiency photon energy up-conversion by an Auger fountain mechanism. Paradoxally, the efficiency of this huge optical non-lineary is due to the importance of a non-radiative recombination path. This observation raises several questions concerning the role of Coulomb forces, k-conservation or non-conservation etc... for Auger or other many-particule interactions at type II interfaces. It also opens unexpected application perspectives, and suggests possible analogies in other fields.

Acknowledgements: we thank T. Lebihen and C. Delalande for their help and the use of their Ti:Sapphire laser, and P. Roussignol for fruitful discussions. LPMC-ENS is UA N° 1437 at CNRS. One of us (WS) is supported by a DAAD PhD fellowship.

references:

° permanent adress: Ioffe Phys. Tech. Inst. RAS, St Petersburg, Russia

1 P. Vagos, P. Boucaud, F.H. Julien, J.M. Lourtioz and R. Planel, Phys. Rev. Lett. 70, 1018 (1993)

2 H.C. Casey and M.B. Panish, Heterostructure Lasers, Academic Press, NewYork (1978)

3 G.G. Zegria and V.A. Kharchenko, Sov. Phys. JETP 74, 173 (1992)

4 A.N. Titkov, G. N. Iluridze, I.F. Mironov and V.A. Cheban, Sov. Phys. Semicond. 20, 14 (1986)

5 M. Potemski, R. Stepniewski, J.C. Maan, G. Martinez, P. Wyder and B. Etienne, Phys. Rev. Lett. 66, 2239 (1991)

6 E. Lugagne-Delpon, J.P. André and P. Voisin, Solid State Comm. 86, 1 (1993)

7 E. Lugagne-Delpon, P. Voisin, M. Voos and J.P. André, Appl. Phys. Lett. 60, 3087 (1992)

8 preliminary observation of this effect was reported by us at the 6th int. Conf. Modulated Semiconductor Structure (Solid State Electronics 37, 1041 (1994))

9 G. Bastard,"wave mechanics applied to semiconductor heterostructures" (les Editions de Physique, Les Ulis, 1988), chap. V. We actually do not measure n_S, but there is little uncertainty in the modeling of the charge transfer.

10 These PLE spectra are obtained using a very low power source consisting of an halogen lamp filtered by a monochromator.

11 M.J. Brasil, R.E. Nahory, W.E. Quinn, M.C. Tamargo and H.H. Farrel, Appl. Phys. Lett. 60, 1981 (1992)

12 G. Benz and R. Conradt, Phys. Rev. B16, 843 (1977)

13 B. Sermage, D.S. Chemla, D. Sivco and A.Y. Cho, IEEE J. Quantum Electronics, QE 22, 774 (1986) and references therein

Figure captions

Fig.1:

(a) Sketch of the band structure of the InP-AlInAs heterojunction. (b) Luminescence spectrum (solid lines) under low power excitation with an He-Ne laser, and excitation spectra (dashed lines) of the various lines[10].(c) Luminescence spectrum with a 20 mW excitation power at $h\nu_2$=1.325 eV, showing the up-converted InP luminescence.

Fig. 2:

Integrated intensities of the interface "A" and InP "B" luminescence lines versus the pump intensity (a) for an excitation energy $h\nu_1$=1.51 eV and (b) for an excitation at $h\nu_2$ =1.325 eV.

Fig. 3:

Calculated absorption spectra using numerical solutions of the Schrödinger equation for the potentials sketched in the insert: ideal heterojunction (a), or heterojunction with an additional 5.6 Å InAs layer at the interface (b), or with a 30 Å wide graded interface (c). The constant $\alpha_0 \approx 6.\ 10^{-3}$ is the absorption by a heavy-hole to electron transition in a type I QW.

Fig. 4:

Ratio of the InP to interface luminescence intensities as a function of the pump power at $h\nu_3$=1.375 eV, under "tight" focusing. The solid line is drawn through the data points, and the dashed and dotted lines are fits using Eqs. 1-4 and slightly different fitting parameters.

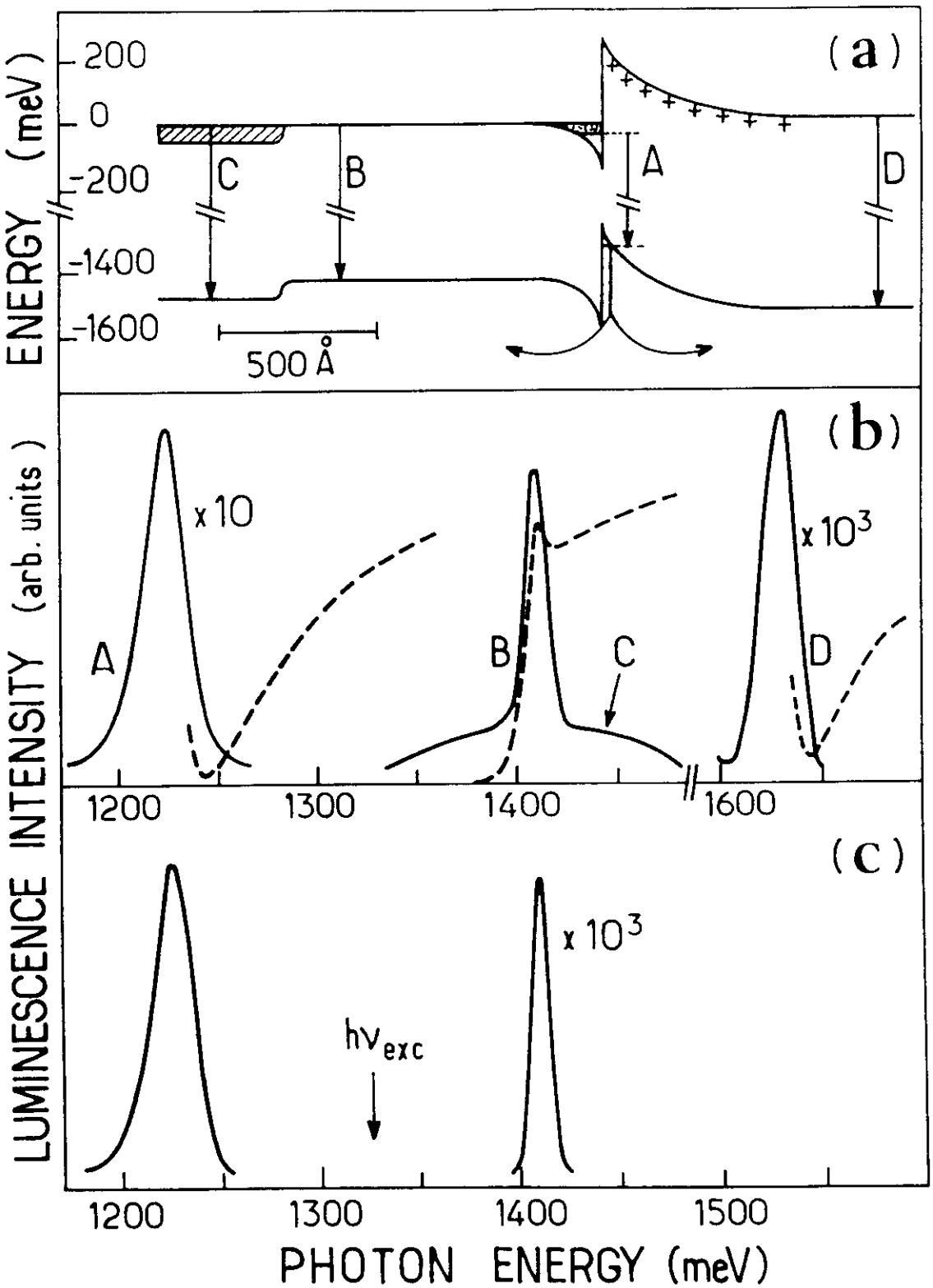
(a)
200
0
-200
-1400
-1600
ENERGY (meV)
C
B
A
D
500 Å
(b)
x 10
x 10³
A
B
C
D
1200
1300
1400
1600
(c)
x 10³
hν exc
1200
1300
1400
1500
LUMINESCENCE INTENSITY (arb. units)
PHOTON ENERGY (meV)

Fig. 1

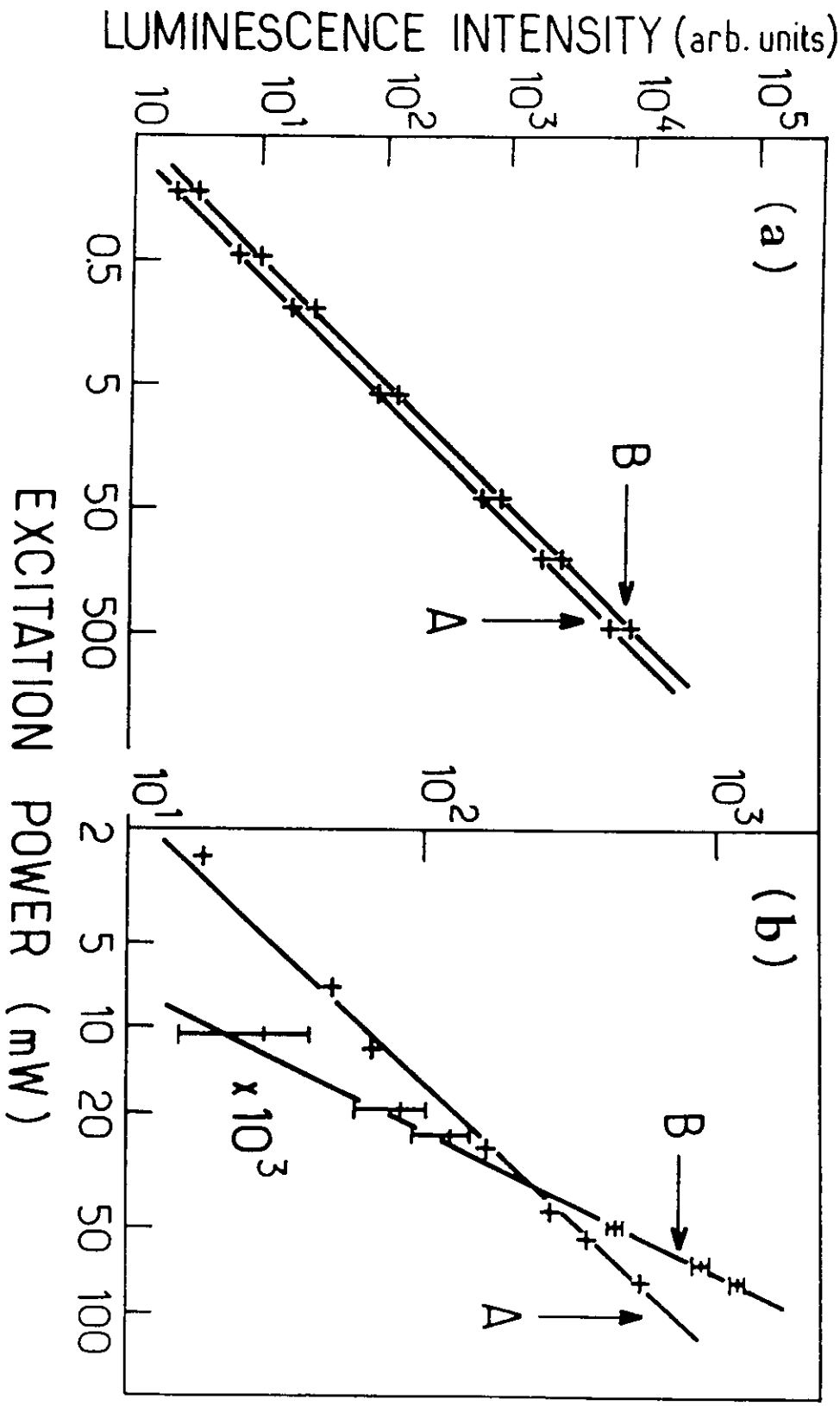
LUMINESCENCE INTENSITY (arb. units)
10
10^1
10^2
10^3
10^4
10^5
(a)
B
A
0.5
5
50
500
EXCITATION POWER (mW)
10^1
10^2
10^3
(b)
x 10^3
B
A
2
5
10
20
50
100

Fig. 2

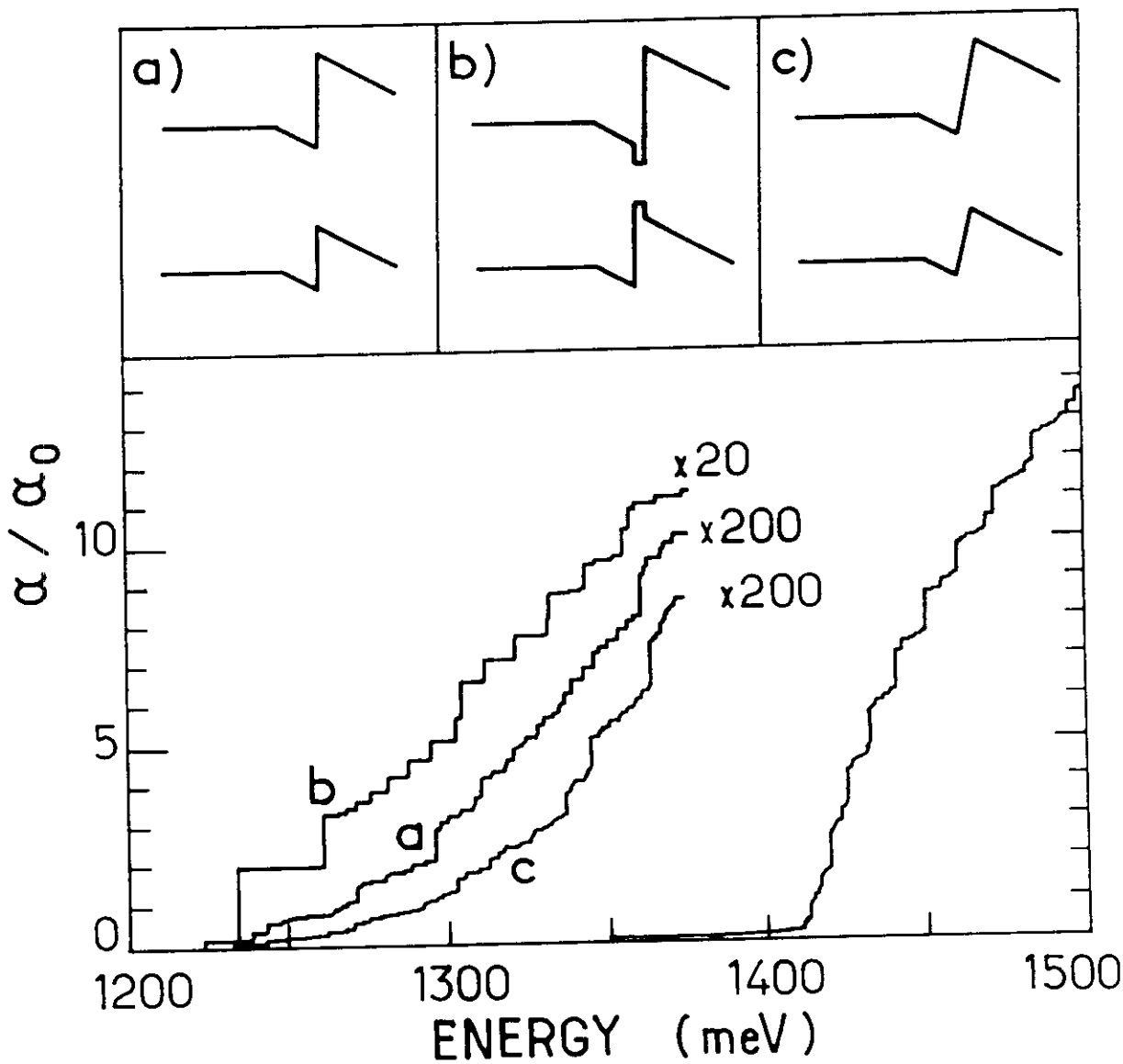

Fig. 3

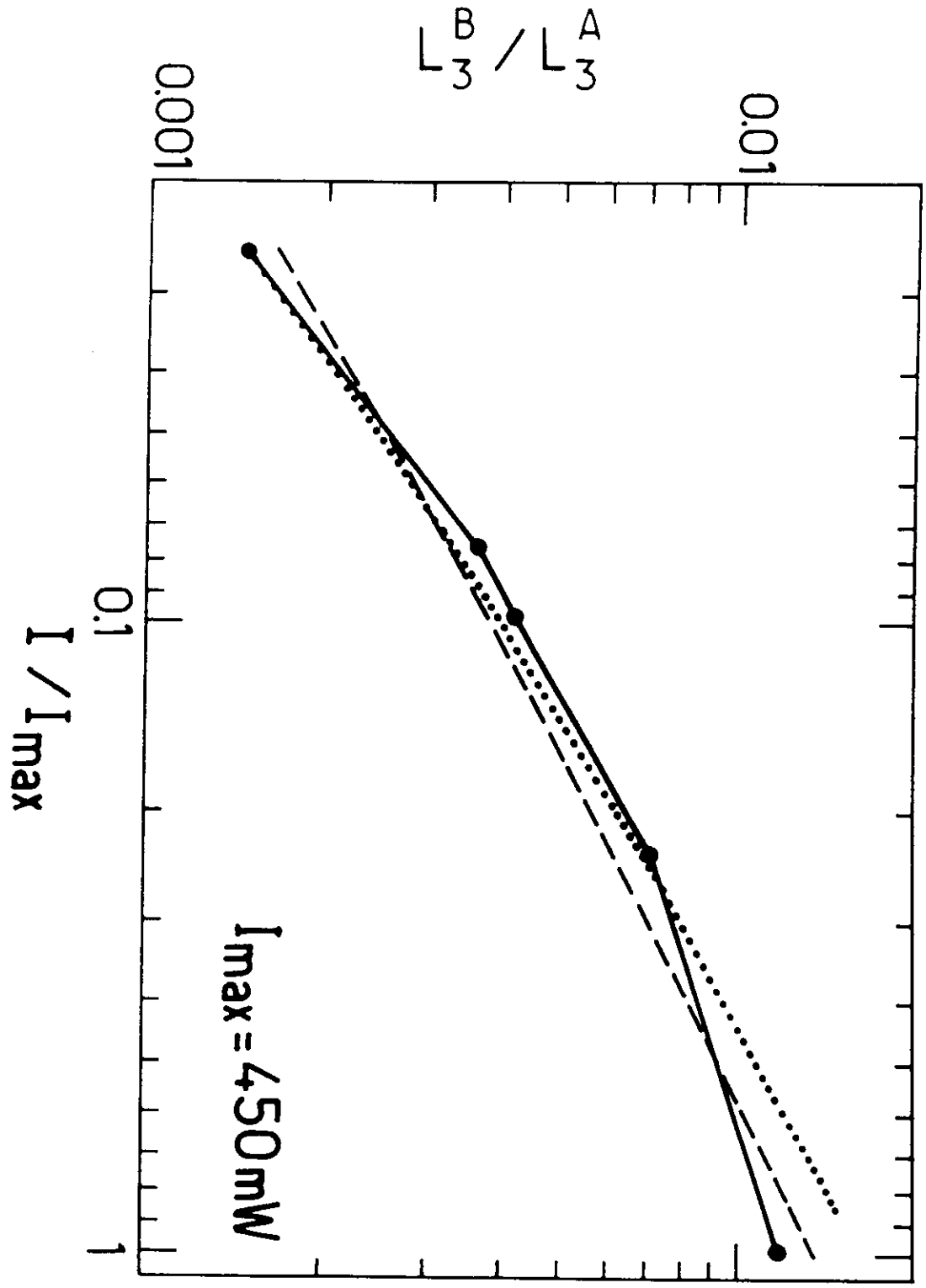

Fig. 4

AG

Low power all-optical bistability in InGaAs-AlInAs superlattices: demonstration of a wireless self-electro-optical effect device operating at 1.5 μm

J. Couturier and P. Voisin

Laboratoire de Physique de la Matière Condensée de l'Ecole Normale Supérieure

24 rue Lhomond, F75005 Paris, France

J.C. Harmand

France-Telecom, Centre National d'Etude des Télécommunications

196 Av. H. Ravera, F 92220 Bagneux, France

We report the observation of optical transmission bistability at low temperature in unprocessed InGaAs-AlInAs superlattice PIN structures. Bistability results, in analogy with the self electro-optical effect device, from a positive feedback mecanism due to the interplay between Wannier-Stark effect, built-in field and screening by photocarriers.

suggested PACS codes: 42.65.Pc, 78.20.Jq, 78.65.Fa

There is a tremendous potential interest in optical bistable devices because they are ideally suited to highly parallel information processing, commutation matrices for telecommunications, etc.. However, all-optical bistables[1] based on non-linear properties of the optical index in Fabry-Pérot cavities require a relatively high power (>> 1μW / μm^2, i.e. more than 1 mW / pixel[2]) which seriously limits cw operation and integration. On the other hand, electro-optical bistables like the self electro-optical effect device[3] (SEED) do function at low power (a few μW / device), but they need an individual electrical circuit, which implies a complex architecture of interconnections and again limits the possibility of large scale integration. Recently, the invention of the S-SEED[4] has open new perspectives since this combination of two SEEDs functions with no other external electrical connection than a simple bias voltage. However, these devices still require rather complex processing[5] and differential illumination which hamper their use in large scale matrices. While the main stream of research in the field of digital optics is presently devoted to "smart pixel" technologies[4-7], we show that all-optical bistability may be obtained at very low power and without any processing in properly designed superlattice *p-i-n* diodes, using the combination of Wannier-Stark effect, built-in electric field and screening.

The sample used in this study is a InGaAs-AlInAs superlattice electro-optical modulator structure grown by Molecular Beam Epitaxy on n^+ InP substrates. It consists in a 20 period InGaAs (60 Å)-AlInAs (20 Å) superlattice embedded between "confinement" layers formed by 10-period InGaAs (25 Å)-AlInAs (20 Å). This undoped structure, originally designed for guided-wave

modulation at 1.55 μm[8], is inserted between thick AlInAs n^+ and p^+ electrodes and forms a *p-i-n* diode. In addition, the sample is topped by a 1000 Å thick p^+ InGaAs contact layer. Low temperature (2 K) photocurrent spectra at 0 V and 0.5 V forward bias are shown in Fig. 1a. These spectra illustrate the now well-known scenario of the Wannier-Stark effect[9-11]: the absorption spectrum of a biased superlattice consists in a series of transitions between discrete quantum states partially localized in the vincinity of the different quantum wells. These transitions occur at the energies E_0 + p eFd, where E_0 is essentially the bandgap of an isolated quantum well, F is the electric field, d the superperiod and p a relative integer. The p = 0 "vertical" transition is field-independent and corresponds to electron and hole wavefunctions centered in the same quantum well, while the field-dependent $p \neq 0$ "oblique" transitions occur between wavefunctions localized near quantum wells separated by p periods. Here, the built-in electric field (≈50 kV/cm) already corresponds to the "large field" regime where only the dominant vertical transition at 935 meV and weak p=-1 and p=+1 oblique transitions at 900 and 970 meV can be observed. When the field is decreased by applying a 0.5 V forward bias, the p=-1 transition is blue-shifted while its oscillator strength increases, and a weak p=-2 transition becomes observable. Near flatband conditions, all these transitions merge and form the superlattice miniband absorption spectrum. It is clear that near 920 meV, there is a region of well contrasted "blueshift" modulation where the absorption decreases when the field strength increases, while near 900 meV there is the region of low drive voltage "redshift" modulation by the oblique transitions used in the guided-wave modulators[8].

Furthermore, the built-in electric field can be screened by photo-carriers.

This is illustrated in Fig. 1b which shows the transmision spectrum at very low power, modulated using an additional illumination by a 0.5 mW He-Ne laser chopped at 75 Hz: this differential transmission spectrum essentially reveals the difference between the large and low field absorption spectra of Fig. 1a. In particular, the "blueshift" modulation region appears as a strong negative peak at 930 meV. This peak corresponds to a 15 % change in the transmitted intensity, which is quite remarkable since the absorption on the two-dimensional plateau above 980 meV is only 20%. Hence, half a mW distributed over the 3x4 mm^2 sample area is sufficient to modulate 75 % of the available absorption.

In the context of optical switching, the blueshift modulation is essential because it provides a positive feedback mechanism which can lead to bistability. Indeed, if we increase the intensity of the weakly absorbed incident beam at 920 meV, more and more photocarriers will be created, which will screen the electric field and increase the absorption: for a sufficient intensity, absorption will cause its own increase, and the system may switch from the weakly absorbing "high field" regime to the highly absorbing near flat-band regime. This actually occurs in our sample, as illustrated in Fig. 2 which shows the transmitted intensity versus the incident intensity at various photon energies: outside the region of blueshift modulation, we get nearly straigth lines, with a slope 1 in the transparency region and a smaller slope in the absorbing region[12]. On the contrary, near 920 meV, the curves show a clear non-linear behavior and a nice hysteresis loop is observed at hv = 920 meV. To the best of our knowledge, the input power at the middle of the loop, 1$\mu W/mm^2$, is smaller by many orders of magnitude than any all-optical bistability threshold ever reported.

The way this device works has strong analogies with the SEED, but also the major difference that no load circuit is needed. In principle, a "load line" may be obtained by writing that the sum of photo- and diffusion-drift currents is zero, which yields:

$$I = \beta (1 - e^{-\alpha d}) I_{in} - I_0 (e^{qV/kT} - 1) = 0 \qquad (1)$$

where V is the voltage across the diode, α the absorption coefficient, d the SL thickness, I_0 and β are numerical constants, and I_{in} the incident power. However, Eq. 1 assumes an ideal diode and becomes uncorrect near flatband conditions where the photocurrent goes to zero instead of being a constant. We actually believe that the photo-voltage across the superlattice is more satisfactorily described by a simple phenomenological expression like:

$$V = V_0 \{1 - \exp(-\gamma \alpha d I_{in})\} \qquad (2)$$

where $V_0 \approx 0.9$ V is the built-in voltage and γ a constant. This expression shows the same linear dependence at low intensity as Eq. 1, but also displays the necessary assymptote at $V=V_0$. It gives the equivalent of a load line in the form:

$$\alpha d = \ln \{V_0 / (V_0 - V)\} / (\gamma I_{in}) \qquad (3)$$

In Fig. 3, we have plotted the $\alpha d(V)$ curves measured directly from the combination of transmission and photocurrent data, for various photon energies, together with the load lines Eq. 3, obtained for increasing values of γI_{in}. It clearly

appears that in the transparency region (hν=905 meV) or far above the bandgap (hν=990 meV) there exists only one intersection describing the only stable state of the system. On the contrary, for hν=921 meV, there is a domain of γI_{in} where three intersections exist. An argument quite similar to the original discussion of Miller et al.[3] proves that the central point is unstable, while the two others correspond to the stable states in the hysteresis loop. Hence, our device is basically a "wireless superlattice SEED".

While our observation of extremely low power all-optical bistability certainly opens new perspectives, we are still far from an operational device for which a number of technical requirements exist. In particular, room temperature operation and larger contrast in the bistability loop are obviously necessary. As for the first point, we have observed that the differential transmission signal saturates at a similar value at low and room temperatures, which means that the modulation depth is similar. The main difference is that a much higher power (≈100 mW) is needed at room temperature. This is certainly because the faster diffusion of carriers at room temperature (as indicated by Eq. 1) and/or the activation of alternative vertical transport mechanisms (possibly associated with extended defects in our "jumbo" diode) decrease the efficiency of screening by photocarriers. This merely amounts to a much smaller factor γ (Eq.2) at 300 K than at 2 K. In this case, our bistable device should also work at room temperature, at the expense of larger input power. Let us stress that the fabrication of more realistic pixels (eg 30 x 30 μm^2) will keep the input power in sub-microwatt range, even if γ is reduced by a factor 100. Finally, it is noteworthy that the use of asymmetric Fabry-Pérot cavities may solve the modulation contrast even more easily than it did for

conventional SEEDs[13].

In conclusion, we have observed very low power all-optical bistability in a wireless superlattice SEED operating at 1.5 μm. As the Wannier-Stark effect is a genuine band effect, these observations should be easily extended to other systems, including GaAs-AlGaAs or large gap II-VI heterostructures. In principle, it should also be possible to design isolated quantum well structures showing the wireless SEED behavior, but the Wannier-Stark effect has a-priori avantages over the Quantum Confined Stark Effect in terms of low field and high modulation contrast.

Acknowledgements: we have benefitted from discussions with Dr. E. Bigan. LPMC-ENS and France Telecom / CNET-Bagneux are Unités Associées at CNRS. This work is supported in part by DRED.

References:

1 H.M. Gibbs, Optical bistability: controlling light with light (Academic Press, New York, 1985)

2 J.L. Oudar, R. Kuszelewicz, B. Sfez, J.C. Michel and R. Planel, Optical and Quantum Electronics 24, S 193 (1992)

3 D.A.B. Miller, D.S. Chemla, T.C. Damen, T.H. Wood, C.A. Burrus, A.C. Gossard and W. Wiegmann, IEEE Journal of Quantum Electronics QE 21,1462 (1985)

4 A. Lentine, H.S. Hinton, D.A.B. Miller, J.E. Henry, J.E. Cunningham and L. M.F. Chirovski, IEEE Journal of Quantum Electronics QE 25,1928 (1989)

5 F.B. McCormick, F.A. Tooley, J.L. Brubaker, J.M. Sasian, T.J. Cloonan, A.L. Lentine, R.L. Morrison, R.J. Crisci, S.L. Walker, S.J. Hinterlong, and M.J. Herron, Optical Engineering 31, 2697 (1992)

6 P. Kiesel, K.H. Gulden, A. Höfler, B. Knüpfer, M. Kneissl, P. Riel, G.H. Döhler, X. WU and J.S. Smith, Appl. Phys. Lett. 62, 3288 (1993)

7 A. Höfler, K.H. Gulden, P. Kiesel, M. Kneissel, B. Knüpfer, P. Riel, G.H. Döhler, G. Tränkle and G. Weimann, Appl. Phys. Lett. 62, 3399 (1993)

8 E. Bigan, M. Allovon, M. Carré and P. Voisin, Appl. Phys. Lett. 57, 327 (1990)

9 J. Bleuse, G. Bastard and P. Voisin, Phys. Rev. Lett. 60, 220 (1988)

10 E.E. Mendez, F. Agullo-Rueda, and J.M. Hong, Phys. Rev. Lett. 60, 2426 (1988)

11 J. Bleuse, P. Voisin, M. Allovon and M. Quillec, Appl. Phys. Lett. 53, 2632 (1988)

12 The slope at hν=1 eV should be 0.8, but there is an additional absorption in the 1000 Å thick InGaAs contact layer, and the transmission is actually smaller.

13 K.K. Law, R.H. Yan, L.A. Coldren and J.L. Merz, Appl. Phys. Lett. 57 1345 (1990)

Figure captions

Fig. 1 (a) Low temperature photocurrent spectra at 0 V (solid line) and 0.5 V forward bias (dashed line) and (b) differential transmission spectrum. The transmission of the low power working light is modulated by a 0.5 mW He-Ne laser chopped at 75 Hz.

Fig. 2 Transmitted versus incident intensities at various photon energies. The vertical axis has been scaled to ensure a slope equal to unity in the transparency region.

Fig. 3 Absorption versus voltage curves (solid lines) for various photon energies and "load lines" deduced from Eq. 3 (dashed lines) for increasing values of the incident power.

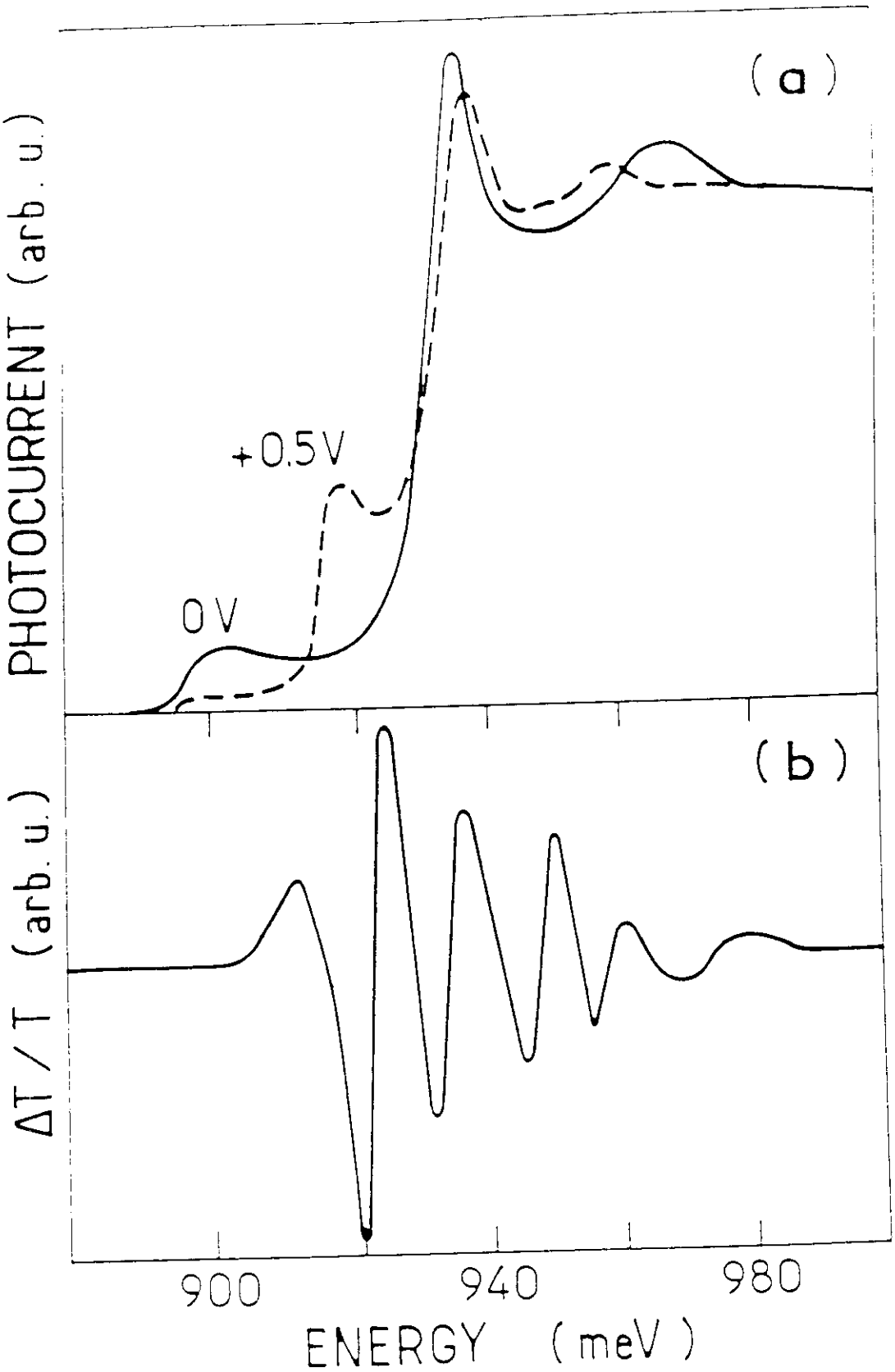

Fig 1

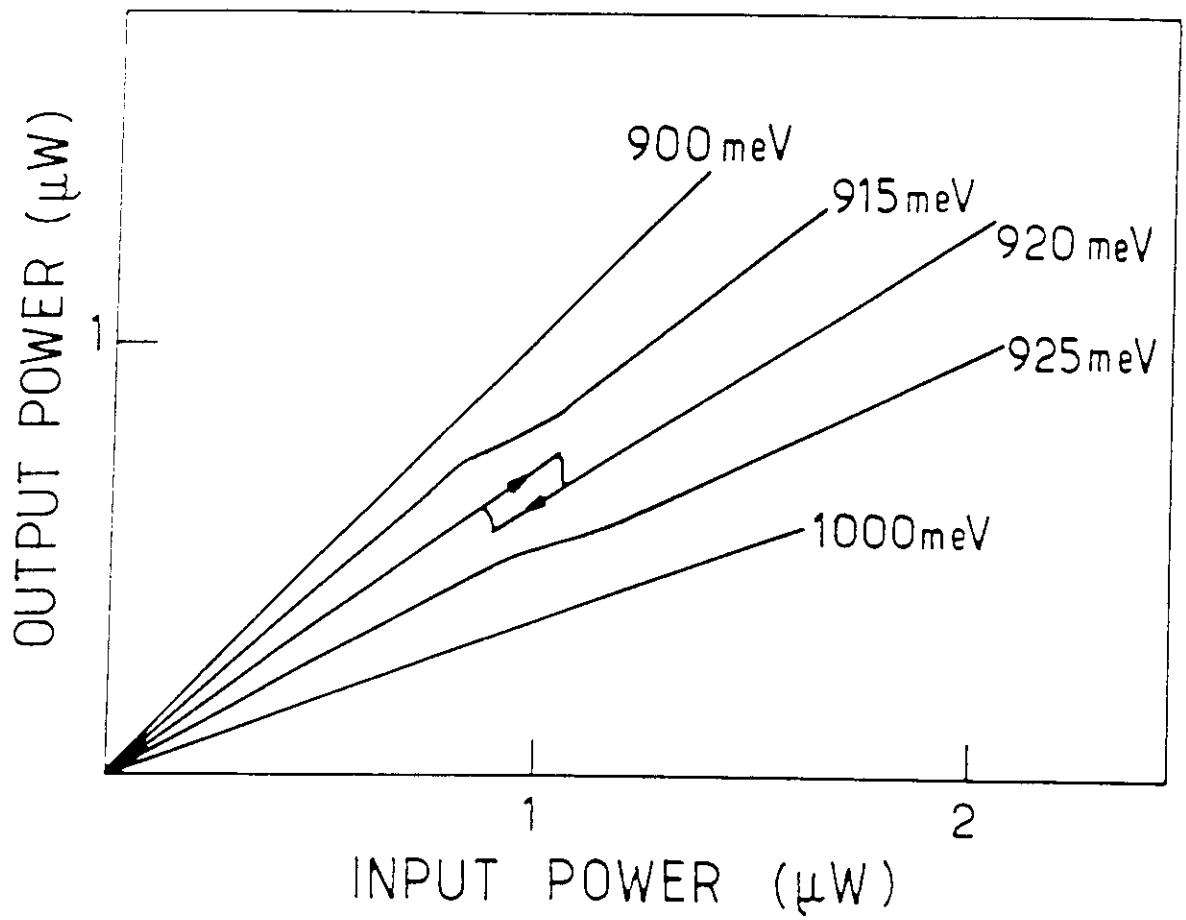
900 meV
915 meV
920 meV
925 meV
1000 meV
OUTPUT POWER (μW)
1
1
2
INPUT POWER (μW)

Fig. 2

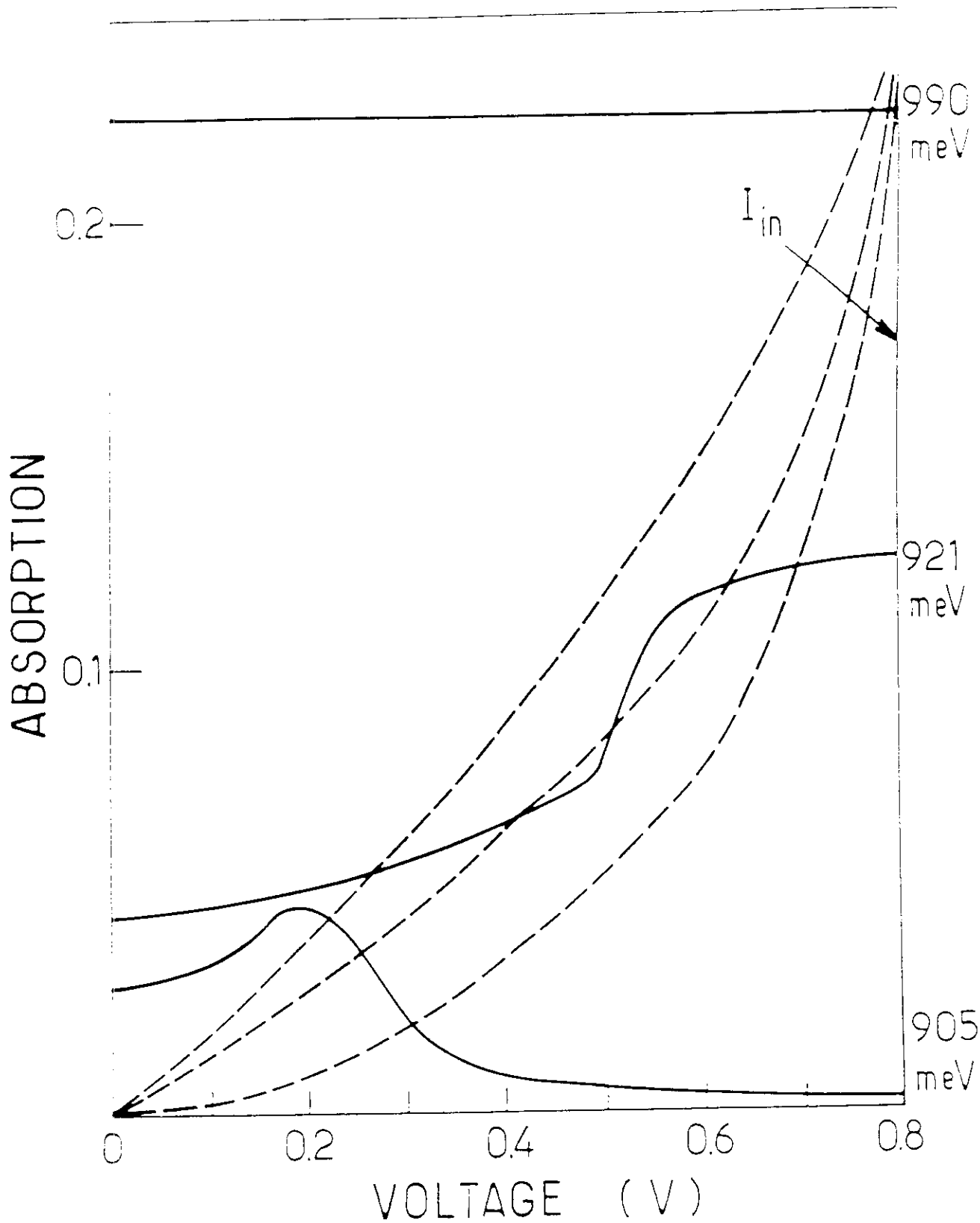
990
meV
I_{in}
0.2
ABSORPTION
0.1
921
meV
905
meV
0
0.2
0.4
0.6
0.8
VOLTAGE (V)

Fig. 3